

## Injection Mechanisms in GaAs Diffused Electroluminescent Junctions

R. C. C. LEITE, J. C. SARACE, D. H. OLSON, B. G. COHEN, AND J. M. WHELAN  
*Bell Telephone Laboratories, Murray Hill, New Jersey*

AND

A. YARIV  
*California Institute of Technology, Pasadena, California*

(Received 25 September 1964)

Injection mechanisms responsible for the electroluminescence in GaAs diffused diodes are studied by examining the behavior of the emission peaks as a function of injection level, doping level, temperature, and depletion-layer widths. Three different injection mechanisms seem to be operative in providing radiation at near-band-gap energies. Models for two of these are proposed and tested. The nature of the third emission remains an open question.

### I. INTRODUCTION

MOST of the recent investigations on the recombination radiation from GaAs  $p$ - $n$  junctions are concerned with the nature of the radiative transitions which follow the injection process.<sup>1-7</sup> In this article we apply ourselves to the injection process itself and present experimental evidence demonstrating the existence of three distinct injection mechanisms in narrow degenerate junctions.

Another purpose of this paper is to fill in the details, both experimental and theoretical, which were, by necessity, left out of two previous short communications.<sup>8,9</sup>

The paper is not concerned with injection processes in general, but only with those processes associated with radiative transitions. The most direct measure of the importance of each injection process is the total (integrated) intensity of the recombination radiation rather than the total current. This is particularly important when a number of injection mechanisms leading to the same or different recombination processes co-exist and/or when, due to the presence of nonradiative processes, the fraction of injected carriers which leads to radiative transitions varies with injection level.

Now a few comments on the correlation between the generated spectra and the externally observed ones. The radiation is generated in a very narrow region near the depletion layer and the wavelength of the emission is

<sup>1</sup> R. N. Hall, G. E. Fenner, J. D. Kingsley, T. J. Sultys, and R. O. Carlson, *Phys. Rev. Letters* **9**, 366 (1962).

<sup>2</sup> M. I. Nathan, W. P. Dumke, G. Burns, F. H. Dill, Jr., and G. J. Lasher, *Appl. Phys. Letters* **1**, 62 (1962).

<sup>3</sup> T. M. Quist, R. H. Rediker, R. J. Keyes, W. E. Kragg, B. Lax, A. L. McWhorter, and H. J. Zeiger, *Appl. Phys. Letters* **1**, 91 (1962).

<sup>4</sup> R. Braunstein, J. I. Pankove, and H. Nelson, *Appl. Phys. Letters* **3**, 31 (1963).

<sup>5</sup> R. F. Shanfele, H. Stutz, J. M. Lavine, and A. A. Iannim, *Appl. Phys. Letters* **3**, 40 (1963).

<sup>6</sup> G. Lucovsky and C. J. Repper, *Appl. Phys. Letters* **3**, 71 (1963).

<sup>7</sup> G. C. Dousmanis, C. W. Mueller, and H. Nelson, *Appl. Phys. Letters* **3**, 133 (1963).

<sup>8</sup> R. C. C. Leite and A. Yariv, Post-deadline paper, American Physical Society meeting, Washington, D. C., 1963 (unpublished).

<sup>9</sup> R. J. Archer, R. C. C. Leite, A. Yariv, S. P. S. Porto, and J. M. Whelan, *Phys. Rev. Letters* **10**, 483 (1963).

very near the absorption edge of the material. As the emitted radiation travels along the material, the spectrum is distorted by a higher absorption in the high-frequency side of the emitted line. A complete correction for this spectral distortion is not always easy because absorption data for different dopings are not easily available and because, due to possible internal reflections, different optical properties within the space charge region, and guiding effects along the junction,<sup>10,11</sup> it is impossible to evaluate properly the effective path traversed by the radiation.

In order to avoid those spectral distortions, we have observed the high-frequency emission by three different methods. (1) Some diodes had most of the  $p$  side removed and a polished gold window permitted most of the radiation to come out from the  $p$  side. In order to avoid back reflection from the  $n$  side (which would reinforce the low-frequency part of the emission),<sup>12</sup> an absorbing  $p$  layer was diffused on the  $n$  side (Fig. 1).

### DIODE STRUCTURE

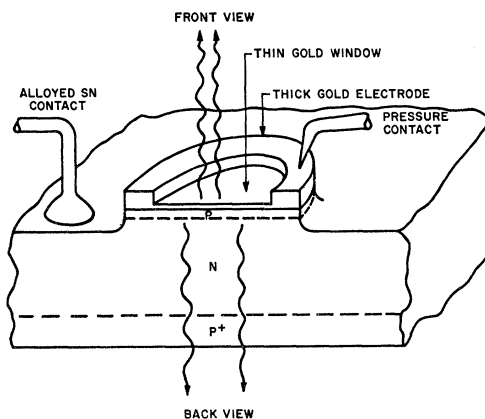


FIG. 1. Diode structure for most of the diodes used in this work.

<sup>10</sup> A. Yariv and R. C. C. Leite, *Appl. Phys. Letters* **2**, 55 (1963).

<sup>11</sup> W. L. Bond, B. G. Cohen, R. C. C. Leite, and A. Yariv, *Appl. Phys. Letters* **2**, 57 (1963).

<sup>12</sup> J. C. Sarace, R. H. Kaiser, J. M. Whelan, and R. C. C. Leite (to be published).

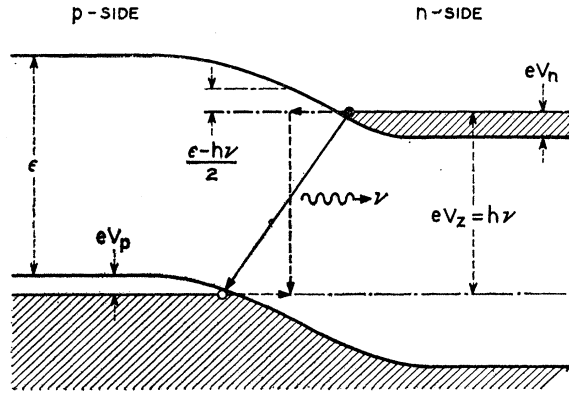


FIG. 2. Diagram for "diagonal tunneling" model.

(2) When absorption data were available for the more uniform  $n$  side and a correction possible, radiation was collected from the  $n$  side. (3) Some spectra were obtained in the direction of the junction where most of the collected light was piped by the waveguide effect.<sup>10</sup> Of course this last method gave less reliable spectra.

## II. RECOMBINATION BY "DIAGONAL" TUNNELING

The possibility of photon assisted tunneling in  $p$ - $n$  junctions has been considered by Aigrain,<sup>13</sup> Sommers,<sup>14</sup> and Pankove.<sup>15</sup> The first direct experimental evidence for this effect was presented by Leite and Yariv,<sup>8</sup> and by Archer and others.<sup>9</sup> The theoretical model proposed in the last two papers consists of a one-step radiative transition from a level in the conduction band in the  $n$  side of the junction to a level in the valence band in the  $p$  side (Fig. 2). The two levels are separated by the energy of the emitted quantum  $h\nu$ . The simultaneous physical translation of the electron and its downgrading in energy can best be described by a diagonal arrow originating in the  $n$  side and terminating in the  $p$  side; hence the word "diagonal" in the title. Most tunneling processes, the one in tunnel diodes for example, involve transitions between states of equal energy and are "horizontal."

Tunneling across the potential hill in a  $p$ - $n$  junction is described by the eigenfunctions of the effective Hamiltonian,

$$\mathcal{H} = -\frac{\hbar^2}{2m_t} \left[ \frac{\partial^2}{\partial x^2} + \frac{\partial^2}{\partial y^2} \right] - \frac{\hbar^2}{2m_l} \frac{\partial^2}{\partial z^2} + V(z), \quad (1)$$

where  $V(z)$  is the potential energy of an electron. " $z$ " is perpendicular to the plane of the junction and is assumed to correspond to the unique axis of the mass ellipsoid, and  $m_t$  and  $m_l$  are the transverse and longitudinal effective masses.

In the adiabatic limit [slow variation of  $V(z)$ ] the eigenfunctions are given by

$$\psi = \psi_u(r) e^{i[k_x x + k_y y + k_z(z)z]}, \quad (2)$$

where  $k_x$  and  $k_y$  are constants and  $k_z(z)$  is given by

$$k_z^2(z) = \frac{2m_l}{\hbar^2} \left\{ E - \left[ V(z) + \frac{\hbar^2}{2m_t} (k_x^2 + k_y^2) \right] \right\}, \quad (3)$$

and  $E$  is the total energy of the electron. The simplified point of view embodied in (3) is sufficient for drawing some basic conclusions. The electrons begin tunneling into the potential  $V(z)$  at a value of  $z$  where  $k_z^2(z)$  goes negative; i.e., when

$$V(z) \geq E - (\hbar^2/2m_t)(k_x^2 + k_y^2). \quad (4)$$

It is clear from (4) that the possession of transverse crystal momentum  $P_t = \hbar(k_x^2 + k_y^2)^{1/2}$  makes it harder for the electron to tunnel. This is equivalent to a reduction of the energy  $E$  by  $P_t^2/2m_t$ , thus causing the classical turning back point to occur earlier. Because of this effect, the tunneling current is carried by electrons with essentially no transverse momentum, i.e., where  $k_x \approx 0$ ,  $k_y \approx 0$ .

The tunneling probability is proportional to the squared magnitude of the matrix element,

$$\mathcal{H}_{cv}' = \int \psi_c(r) \exp[i\mathbf{k}^c(r) \cdot \mathbf{r}] P \times \psi_v^*(r) \times \exp[-i\mathbf{k}^v(r) \cdot \mathbf{r}] dV, \quad (5)$$

where  $P$  is the momentum operator,  $\psi_c(r)$  and  $\psi_v(r)$  are the  $k=0$  wave functions for the conduction and valence bands and  $\mathbf{k}^c(r)$  and  $\mathbf{k}^v(r)$  are the wave vectors.

The conservation of crystal momentum  $\mathbf{k}^v(r) = \mathbf{k}^c(r)$  is usually necessary in order to insure that  $\mathcal{H}_{cv}'$  is not zero. In our case the situation is altogether different. Since  $\psi_v$  and  $\psi_c$  are each localized in opposite sides of the junction, and since  $k_z^c(z)$  and  $k_z^v(z)$  become imaginary at some point (not the same for both), the " $z$ " integration does not require conservation of the " $z$ " crystal momentum. The only nonvanishing contribution to the " $z$ " integration is from the overlap region where  $\exp\{i[k_z^c(z) - k_z^v(z)]\}$  is real. The " $x$ " and " $y$ " integration does require conservation of transverse momentum, but as noted earlier the transverse momentum is zero for the tunneling electrons, so that the transverse momentum is conserved trivially. It is on this basis that the necessity for invoking the conservation of momentum and tunneling via virtual states, as was done by Pankove,<sup>15</sup> was questioned.<sup>8,9</sup>

Furthermore, at high levels of degeneracy, the band edges should be distorted to a point where states near the band edge would not be represented any more by one single-wave function, but rather, by a superposition of wave functions with different  $\mathbf{k}_i$ , where  $\mathbf{k}_i$  are the wave numbers for the unperturbed states near the band

<sup>13</sup> P. Aigrain (private communication).

<sup>14</sup> H. S. Sommers, Jr., Phys. Rev. **124**, 1101 (1961).

<sup>15</sup> J. I. Pankove, Phys. Rev. Letters **9**, 283 (1962).

edges. Thus, the  $\mathbf{k}$  selection rule is not expected to hold at high dopings. This is supported by the observation that a certain phonon satellite content at lower dopings is sometimes present,<sup>16</sup> but never for  $N_D > 5 \times 10^{16} \text{ cm}^{-3}$ .

With a few approximations, it is possible to predict certain experimentally verifiable consequences of the tunneling model proposed above.

The tunneling probability for each carrier is given by Keldish<sup>17</sup> as

$$\pi_z = \exp[-\alpha \epsilon_z^{3/2}/E], \quad (6)$$

where  $\alpha = \pi m^{1/2}/2eh$ ,  $m$  is the tunneling mass,  $E$  is the electric field in the junction, and  $\epsilon_z$  is the energy barrier against which the electrons tunnel. We can use Eq. (6) to calculate the probability for an electron and a hole to tunnel to midjunction. Under completely symmetric (equal doping, equal masses) conditions the integrand in (5) will be symmetric and will peak at midjunction. The value of the integrand at midjunction will thus be proportional to the product of the tunneling probabilities for holes and electrons to that point. From Fig. (2) we see that the potential barrier for midjunction tunneling is

$$\epsilon_z = \frac{1}{2}(\epsilon - h\nu), \quad (7)$$

where  $\epsilon$  is the forbidden gap in eV, which, for  $V_n + V_p \ll \epsilon/e - V$ , becomes

$$\epsilon_z \cong \frac{1}{2}e(V_i - V), \quad (8)$$

where  $V$  is the applied voltage and where  $V_i = \epsilon/e + (V_p - V_n)$  is the built-in potential.

We shall take the electric field  $E$  as the maximum field inside the junction which for a step junction is

$$E_m = 2(V_i - V)/W, \quad (9a)$$

and for a linearly graded junction is

$$E_m = \frac{3}{2}(V_i - V)/W, \quad (9b)$$

where  $W$  is the junction width, and as a function of the applied potential takes the forms

$$W = W_1'(V_i - V)^{1/2} \quad (10a)$$

and

$$W = W_1(V_i - V)^{1/3} \quad (10b)$$

for the step and linearly graded junctions, respectively, and where  $W_1$  and  $W_1'$  are the width constants.

Now, if we take the tunneling mass  $m$  for the simultaneous tunneling as given by

$$1/m = 1/m_e + 1/m_h,$$

and assume that the integrated light intensity  $\mathcal{I}$  is proportional to  $\pi_z^2$ , we have

$$\mathcal{I} \sim \pi_z^2 = \exp[-2\alpha \epsilon_z^{3/2}/E], \quad (11)$$

<sup>16</sup> R. C. C. Leite, J. C. Sarace, and A. Yariv, Appl. Phys. Letters 4, 67 (1964).

<sup>17</sup> L. V. Keldish, Zh. Eksperim. i Teor. Fiz. 34, 962 (1958) [English transl.: Soviet Phys.—JETP 7, 665 (1958)].

and by using (8), (9), and (10) we obtain

$$\mathcal{I} \sim \exp[-(e/2)^{3/2}\alpha W_1'(V_i - V)], \quad (12a)$$

and

$$\mathcal{I} \sim \exp[-(\frac{3}{2})(e/2)^{3/2}\alpha W_1(V_i - V)^{5/6}] \quad (12b)$$

for step and linearly graded junctions, respectively.

Thus, a semilog plot of integrated light intensity against voltage gives for a step junction a straight line with a slope

$$S_T = (e/2)^{3/2}\alpha W_1' = \alpha_1 W_1', \quad (13a)$$

and for a linearly graded junction

$$S_T = (10/9)(e/2)^{3/2}\alpha W_1(V_i - V)^{-1/6} = \alpha_1' W_1. \quad (13b)$$

We have used the tunneling model to predict an exponential dependence of the radiation on the applied voltage.<sup>18</sup> We have, furthermore, derived an expression for the magnitude of the logarithmic slope which is subject to direct experimental test.

Another consequence of the tunneling model becomes clear from a study of Fig. 1. Since only electrons and holes very near the quasi-Fermi levels have an appreciable probability of tunneling (these carriers have the smallest barrier  $\epsilon_z$  against which to tunnel), it follows that the applied voltage  $V$  and the peak radiation frequency  $\nu_p$  are related by

$$h\nu_p = eV. \quad (14)$$

Equation (14) holds when only electrons and holes at the quasi-Fermi levels are considered and for temperatures low enough so that the "fuzziness" of the Fermi tails can be ignored. An exact calculation will show that the decreasing tunneling probability of electrons (and holes) below the electron quasi-Fermi level in the conduction band (above the hole quasi-Fermi level in the valence band) is compensated, up to a point, by the larger density of these carriers. These will cause the peak emission to shift to lower frequencies by an amount  $eV_0/h$  so that the expected relation between  $V$  and  $\nu$  is

$$h\nu_p = e(V - V_0). \quad (15)$$

In summary, the diagonal tunneling model predicts an emission band whose peak frequency increases linearly with applied voltage, and has an exponential increase in integrated intensity with voltage. The latter proportionality factor, given by Eq. (13), can be calculated from known or readily measured quantities. These features will be compared with those of observed injection luminescence bands in Sec. IV.

### III. THE BAND-FILLING MODEL

The experimental evidence to be discussed in Sec. IV shows that in certain cases the measured logarithmic slope  $S$  and its dependence on the diode parameters does

<sup>18</sup> A similar procedure was used by A. G. Chynoweth, W. L. Feldman, and R. A. Logan [Phys. Rev. 121, 684 (1961)] in investigating the excess current in silicon Esaki junctions.

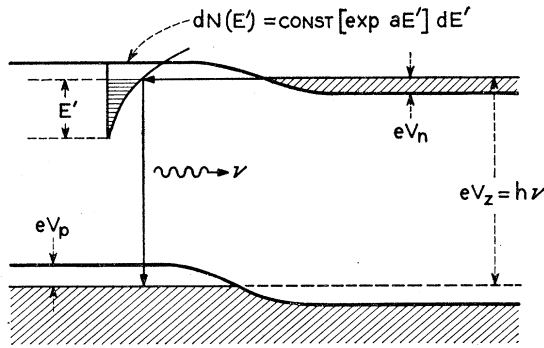


FIG. 3. Diagram for the "band filling model."

not always agree with the diagonal tunneling model. In these cases the data are usually consistent with the band-filling model. According to this model, the high impurity concentration spoils the sharpness of the forbidden gap edges and causes the latter to tail off into the gap.<sup>19</sup>

Gershenzon *et al.*<sup>20</sup> first proposed this model to explain the observed shift of the peak emission frequency with current. Archer *et al.*<sup>9</sup> have shown that the model was also consistent with the observed exponential dependence of the integrated light intensity on  $V$ . We shall show below that when the band to be filled is exponential, both these observations as well as the dependence of the peak emission frequency  $\nu_p$  on  $V$  are not sufficient to distinguish between band filling and the occurrence of direct diagonal tunneling.

The model is illustrated by Fig. 3 in which, for the sake of simplicity we show the case for electron injection only. Under forward bias conduction band electrons from the  $n$ -type side are injected into the band tail of the conduction band in the  $p$  side. This spatial translation of electrons is taken to be *horizontal*, i.e., without appreciable change in energy of the injected carriers. This is necessary in order to account for the experimentally observed relationship

$$e(V - V_0) = h\nu_p$$

relating the peak emission frequency  $\nu_p$  and the applied voltage  $V$ . In contrast with the case of "diagonal tunneling" details of injection cannot be inferred from the slope  $S_B$  of  $\log \mathcal{G}$  versus  $V$  since in order to have filling of the band tail the rate must be recombination controlled. Thus,  $S_B$  is now determined by the density of states function  $N(E)$  of the band tail, and should not be temperature-dependent.

Whether injection takes place through impurity states by a multistep tunneling process<sup>20</sup> or by simple horizontal tunneling<sup>9</sup> or just by diffusion through an impurity band cannot be determined by the present technique. For simplicity we shall call this process

<sup>19</sup> J. I. Pankove and P. Aigrain, *Phys. Rev.* **126**, 956 (1962).

<sup>20</sup> D. F. Nelson, M. Gershenzon, A. Ashkin, L. A. D'Asaro, and J. C. Sarace, *Appl. Phys. Letters* **2**, 182 (1962).

"horizontal tunneling." Referring to Fig. 3 we show that at a given applied voltage  $V$  the impurity band is filled up to a level  $E$ . Since tunneling is energy conserving and since it cannot occur into impurity states which are already occupied it follows that  $E$  and the quasi-Fermi level for electrons on the  $n$  side are at the same energy level, as shown in Fig. 3.

If the density of states in the impurity band is given by

$$dN(E) = \text{const} \times [\exp(aE)] dE,$$

and if we further assume a recombination lifetime  $\tau$  which is independent of  $E$  we have

$$\mathcal{G} = \text{const} \times e^{ah\nu_p}, \quad (16)$$

where we assume that peak radiation at  $\nu_p$  is due to electrons near the (filled) top, i.e., at  $E$  which explains the observed shift of  $\nu_p$  as a function of the integrated intensity.<sup>9</sup>

A second consequence of this model is due to the assumption of band filling by "horizontal tunneling." This, as noted earlier, forces  $E$  and the quasi-Fermi level on the  $n$  side to coincide in energy, so that from Fig. 3 we have

$$h\nu_p = eV, \quad (14)$$

if it is assumed that  $\nu_p$  is due to electrons near  $E$ . In reality, owing to diffusion following injection and also to the fact that recombination takes place between holes and electrons distributed over a finite energy range, the peak energy  $h\nu_p$  will be displaced toward lower energies and (14) becomes

$$h\nu_p = e(V - V_0). \quad (17)$$

One expects the electron concentration in the  $p$  side to decrease with distance from the junction. This would only affect the shape of the emission band and not relations (16) and (17) as long as the law that describes the electron concentration as a function of distance from the junction does not change with injection level. If electrons recombine with holes that have a weakly energy-dependent distribution, and if the electron concentration decreases exponentially with distance from the junction, then the energy of the peak emission band  $h\nu_p$  is given by

$$h\nu_p = e(V + V_p) - (1/a) \quad (18)$$

and the shape of the emission band is described by its slope

$$dJ/d(h\nu) = a - [e(V + V_p) - h\nu]^{-1}, \quad (19)$$

where  $J$  is the relative intensity at  $h\nu$ .

In summary, we note that if one assumes an exponential band filled by "horizontal" tunneling injection, it follows that:

(a) An exponential dependence of  $\mathcal{G}$  on  $\nu_p$  obtains, with a temperature-independent logarithmic slope.

(b) An equality (in the sense of 17) between  $h\nu_p$  and  $eV$  obtains.

TABLE I. Diodes characteristics:  $N_D$ =donor concentrations;  $C_0$ =acceptor concentration at the diffusing surface;  $n_{285}n_{77}$ =external efficiencies at 285° and 77°K;  $W_0$ =zero bias depletion layer width;  $\gamma$ =measured impurity gradient;  $T$ =diffusing temperature.

Diode (No.)	$N_D$ (cm <sup>-3</sup> )	Donor	$T$ (°C)	$C_0$	$n_{(285)}$ (%)	$n_{(77)}$ (%)	$W_0$ (Å)	$\gamma$
1	$2 \times 10^{18}$	Te	800	$> 10^{20}$	...	...	900	...
2	$2 \times 10^{18}$	Te	650	$5 \times 10^{19}$	0.1	2.5	274	$4.2 \times 10^{24}$
3	$2 \times 10^{18}$	Te	750	$> 10^{20}$	...	...	377	...
4	$2 \times 10^{18}$	Te	750	$> 10^{20}$	0.046	0.34	467	...
5	$3.2 \times 10^{17}$	Te	650	$5 \times 10^{19}$	...	...	775	...
6	$3 \times 10^{17}$	Te	650	$5 \times 10^{19}$	0.043	0.24	957	$9.5 \times 10^{22}$
7	$2 \times 10^{18}$	Te	750	$4 \times 10^{18}$	0.03	1.5	2,500	$6 \times 10^{21}$
8	$4 \times 10^{15}$	S	650	$5 \times 10^{19}$	...	...	4380	...
9	$2 \times 10^{18}$	Te	750	$6 \times 10^{18}$	0.02	2.15	1240	...
10	$2 \times 10^{18}$	Te	800	$3 \times 10^{18}$	...	1.6	1300	$8 \times 10^{21}$
11	$2.3 \times 10^{16}$	S	700	$> 10^{20}$	0.01	0.64	3100	...
12	$1.2 \times 10^{18}$	Te	850	...	0.019	1.0	985	$9.5 \times 10^{22}$
13	$5 \times 10^{17}$	Te	750	$5 \times 10^{19}$	0.020	1.2	1300	...
14	$6 \times 10^{16}$	Te	700	$5 \times 10^{19}$	...	...	1250	...

Conclusions (a) and (b) were seen to result also from the tunneling model of Sec. II. It follows that in order to determine which of the two mechanisms prevails in a given emission, we need some additional information. The distinction between the two injection mechanisms is based on the observed dependence of the logarithmic slope  $S$  on the junction width constant  $W_1$  and on the  $n$  concentration. This point and the related experimental evidence will be discussed in Sec. V.

#### IV. EXPERIMENTAL NOTES

The GaAs used in these experiments was float zone refined with ten passes and then selectively doped with either Te, S, or Se. Slices were cut perpendicular to the growth direction (100), and chemically polished with  $\text{CH}_3\text{OH}$ ,  $\text{Br}_2$ , prior to the junction introduction by Zn diffusion. Two diffusion sources were used to provide a range of junction depths and space charge widths. These were ZnO-GaAs (sealed ampoule) and Zn-Ga (open-box-type diffusion). Table I describes the junction parameters of the diodes selected for this work.

Contacts to the diode were made by alloying tin to the  $n$ -type GaAs and depositing W plus electroplated gold to the diffused layer. To obtain the spectrum radiating through the diffused layer, a few diodes were made with a small area of the  $p$  contact removed and replaced with a thin (approximately 200 Å) gold film.

The diffused diodes were mounted in cryogenic Dewars making it possible to perform the experiments down to 1.2°K. The exciting forward diode current was square-pulsed electronically with a duty cycle of 50%. The resulting emission was passed through a grating monochromator and detected by an S-1 photomultiplier cooled to "dry ice" temperature. The output of the photomultiplier was fed into a phase synchronous detector synchronized by the current chopping signal. The output was then recorded on a strip chart recorder whose horizontal drive was calibrated by markers generated by the monochromator wavelength drive. Output was observed down to a few tenths of micro-

amperes (0.2 mA/cm<sup>2</sup>) of biasing current. It is interesting to note that at this point the quantum efficiency was vanishingly small so that the detection sensitivity was far in excess of what may be indicated by a linear extrapolation from measurements at high injection levels, where the quantum efficiency is near unity.

#### V. DISCUSSION OF EXPERIMENTAL RESULTS

Most of the diodes investigated displayed two distinct straight line regions in a plot of  $\log \mathcal{J}$  versus  $V$ . At low injection levels, the curve possesses a slope which we denote as  $S_T$  and at higher injection levels a larger slope  $S_B$ . The temperature independence of both slopes as well as the observation that the peak emission satisfies a relation of the form  $h\nu = e(V - V_0)$ , suggests that we deal with two different tunneling mechanisms.

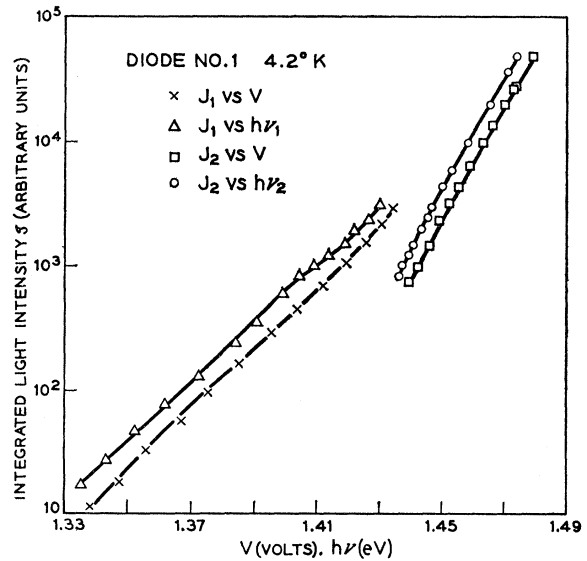


FIG. 4. Integrated light intensity versus voltage and emission peak energy characteristics. (Peak energy corrected for overlap of the two emission peaks.)  $J_1$  belongs to the "fast" moving peak,  $J_2$  to the "slow" peak.

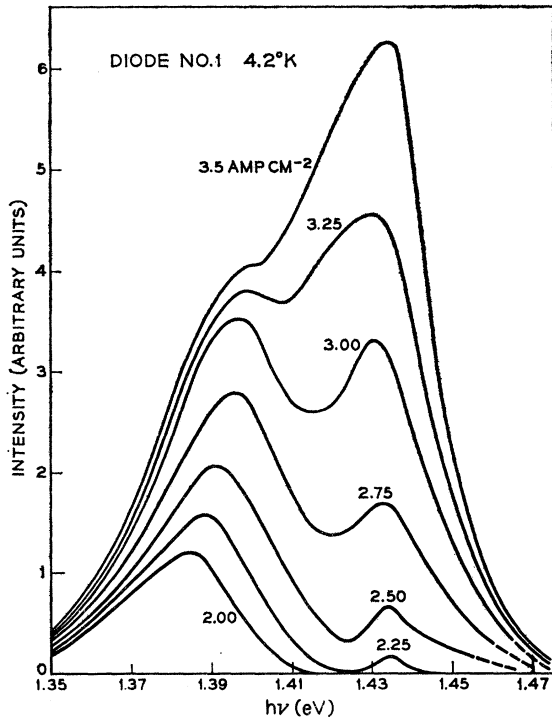


FIG. 5. Spectral development in the "transition region" at 4.2°K.

Some diodes, besides those "moving" peaks displayed one or two stationary peaks that we shall describe further in this section.

The data from a series of diodes, all prepared from a single *n*-type substrate are shown in Figs. 4, 5, and 6.

Figure 4 shows a  $\log \mathcal{J}$  versus  $V$  and a  $\log \mathcal{J}$  versus  $h\nu/e$  plot for one of those diodes. Figures 5 and 6 show the evolution of the spectra at different injection levels in a current range that we shall call the "transition region." Figure 5 refers to 4.2°K and Fig. 6 to 77°K. The spectra at 20°K are similar to the one at 4.2°K. A plot of the emission intensity versus frequency, as in Fig. 5, shows only two emission peaks (beside the low energy emission at  $\sim 1$  eV) from 4.2 to 77°K. At low injection levels (from 1 mA/cm<sup>2</sup> up to  $\sim 200$  mA/cm<sup>2</sup>) only one emission is seen whose peak frequency is shifting rapidly as the current is varied. We shall refer to this peak as the "fast" peak. At injection levels around 200 mA/cm<sup>2</sup> a second emission begins to show up. The peak frequency for this emission shifts slowly as the current is increased and the emission is thus a "slow" moving one. Over a range of injection levels between 2.0 A/cm<sup>2</sup> and 4.0 A/cm<sup>2</sup>, both peaks can be seen simultaneously. At high injection levels, the "slow" moving peak contains most of the emitted radiation so that the "fast" peak eventually becomes buried in its tail and can no longer be resolved. In most of the samples we dealt with, the "fast-slow transition" is not easily observed except by the slope change, but in most cases careful observation

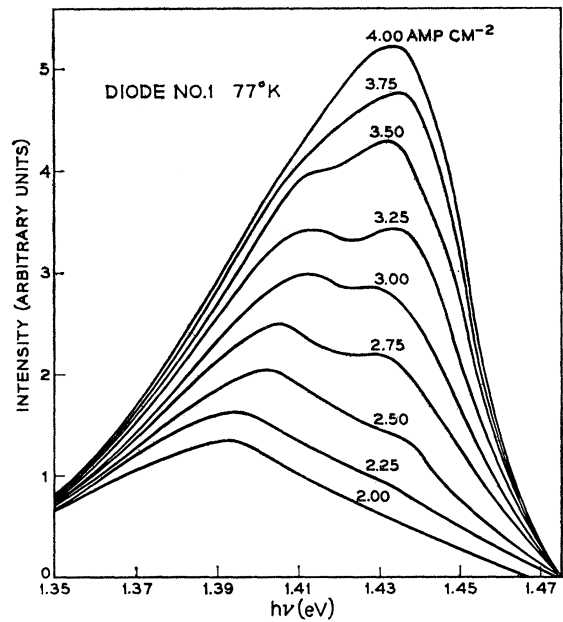


FIG. 6. Spectral development in the "transition region" at 77°K.

reveals a slight broadening of the emission in the "transition region."

A series of  $\log \mathcal{J}$  versus  $V$  curves for low injection currents ("fast peaks") for different depletion layer widths  $W$  is shown in Fig. 7. Capacitance measurements have been performed in order to determine the junction characteristics and this is summarized in Table I. Figure 7 includes both abrupt and linearly graded junctions. It is seen from this figure that the same emission peak frequency may, in thin junctions with small  $S_T$ , shift with current as much as 300 meV. As an impurity band that wide is very unlikely to occur one has

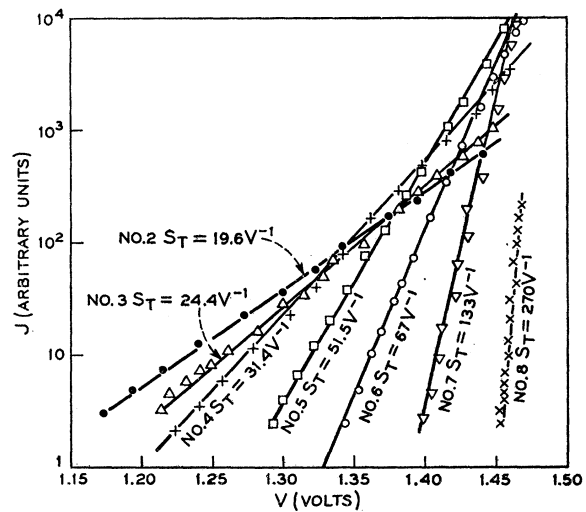


FIG. 7. Plot of integrated light intensity  $J$  versus applied voltage  $V$  for several diodes at low injection levels when "diagonal tunneling" is the only injection mechanism present.

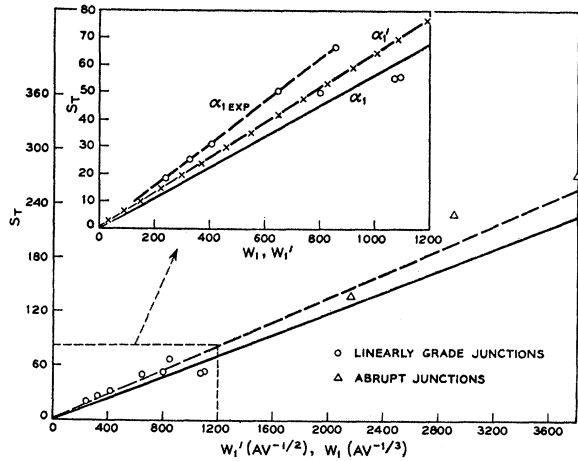


FIG. 8. Plot of the slope  $S_T$  (fast moving peak) as a function of the width, constants  $W_1$  and  $W_1'$ .  $\alpha_1$  and  $\alpha_1'$  are the theoretical curves for abrupt and linearly graded junctions.

to resort to a displacement of the level in which the transition originates with respect to the terminating level which is consistent with "diagonal tunneling."

Figure 8 shows a plot of the measured slope  $S_T$  as a function of the width constant  $W_1$ . This is calculated by means of Eqs. (10), where  $V_i$  and  $W_0$  are obtained from capacitance measurements. This figure includes theoretical curves  $S_T = S_T(W_1)$ , both for abrupt and linearly graded junctions. Those were calculated by means of relations (13) where we have used  $m = 0.1m_0$ .

One notices that the experimental points  $S_T = S_T(W_1)$  fall on a straight line for  $W_1 < 1000 \text{ \AA V}^{-1/3}$ , in good agreement with the "diagonal" tunneling model even though this curve deviates slightly from the theoretical one. This is hardly surprising in view of the many approximations in the model.

Deviations become important for  $W_1 > 1000 \text{ \AA V}^{-1/3}$ , but for linearly graded junctions with  $W_1 > 2000 \text{ \AA V}^{-1/2}$  agreement is again satisfactory. Figure 9 is a plot of the slopes  $S_B$  (slow moving peaks) as a function of the donor concentration  $n$ . The monotonic decrease of  $S_B$  as a function of  $n$  is consistent with an impurity band filling model and suggests that this band is related to donor impurity rather than to acceptor impurity states.

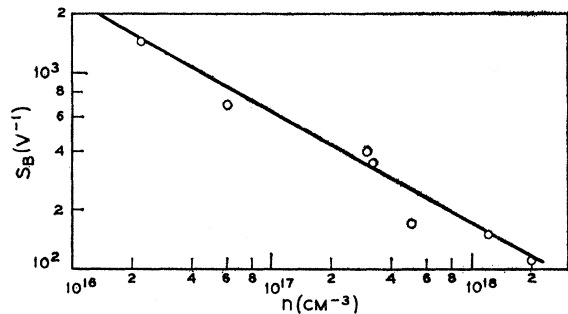


FIG. 9. Plot of the slope  $S_B$  (slow moving peak) as a function of donor concentration  $n$ .

The recombination occurs on the  $p$  side and probably involves acceptor states, as demonstrated by Nathan *et al.*<sup>21</sup> by direct comparison of  $p$ - $n$  electroluminescence with  $p$  and  $n$  photoluminescence.

In summary the differentiation between the two tunneling mechanisms is based on the dependence of the logarithmic slopes of the  $\mathcal{I}$  versus  $V$  curves on  $n$  and  $W_1$ .  $S_T$  varies linearly with  $W_1$  as expected and has the right order of magnitude.  $S_B$  does not depend on  $W_1$  but decreases with increasing  $n$  which is to be expected from a band-filling model.

A third injection mechanism must be ascribed to "stationary" emission peaks, i.e., emissions which do not shift with the injection level and consequently, their peak intensities do not obey a relation of the form  $h\nu_p = e(V - V_0)$ . Stationary peaks were first reported by Leite *et al.*<sup>16</sup> and Sarace *et al.*<sup>22</sup> for zone-floated GaAs. We have since observed several "stationary" peaks whose energies ranges from 1.47 to 1.511 eV at 4.2°K. Their energy and existence depend on the nature of the donor and its concentration. At high injection levels they are dominated by the moving peak in diodes where  $n$  is higher than  $10^{17}$ , but for lower donor dopings they may become prominent at temperatures  $> 77^\circ\text{K}$ .

Figure 10 shows the spectra at 4.2°K for a "low" donor concentration ( $n = 2 \times 10^{16}$ ) diode, at three different injection levels.

At low current densities ( $J < 1.0 \text{ Acm}^{-2}$ ) the only emission peaks present are  $\nu_1$  (1.511 eV) and  $\nu_2$  (1.491 eV). At  $\sim 2 \text{ Acm}^{-2}$ ,  $\nu_3$  and its phonon satellite  $\nu_4$  appear. With increasing  $J$ ,  $\nu_3$  shifts toward  $\nu_2$  and  $\nu_1$ .  $\nu_2$  first becomes buried in  $\nu_3$  (for  $J \simeq 4.0 \text{ Acm}^{-2}$ ) as shown in Fig. 10(b). Then  $\nu_1$  also disappears in the high-energy wing of  $\nu_3$  (for  $J > 40 \text{ Acm}^{-2}$ ), as shown in Fig. 10(a). This same diode nevertheless had  $\nu_1$  as the dominant emission from 77°K (at 1.508 eV) to room temperature. The dependence of intensity on temperature suggests that the injected carriers responsible for  $\nu_1$  are "frozen

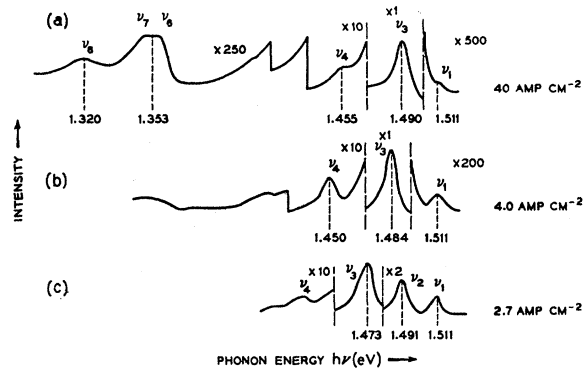


FIG. 10. Electroluminescence spectra of a low donor concentration ( $n = 2 \times 10^{16} \text{ cm}^{-3}$ ) diode at different injection levels.

<sup>21</sup> M. I. Nathan and G. Burns, Appl. Phys. Letters 1, 89 (1962), also Phys. Rev. 129, 125 (1963).

<sup>22</sup> J. C. Sarace, R. H. Kaiser, J. M. Whelan, and R. C. C. Leite (to be published).

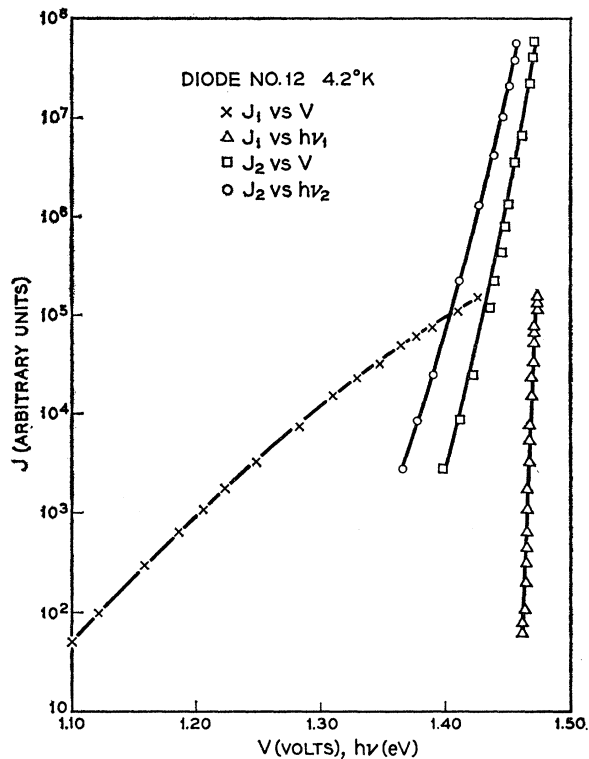


FIG. 11. Integrated light intensity versus applied voltage and peak-energy characteristics at 4.2°K for a diode in which one of the emission peaks is such that  $h\nu - eV > 1000kT$  at low injection levels.

out" at low temperatures. The coincidence of  $\nu_1$  peak emission energy with the peak emission of photoluminescence data in  $n$  material<sup>21</sup> suggests that  $\nu_1$  originates in the  $n$  side following hole injection.

An important observation is the fact that at low injection levels  $h\nu_1 - eV > 100kT$ . Figure 11 shows a plot of  $\mathcal{J}$  versus  $h\nu$  and  $J$  versus  $V$  for a diode that displayed two emissions, one "quasistationary" peak around 1.47 eV and the other a moving peak. For this particular diode the 1.47-eV peak (at 4.2°K) is such that  $h\nu_1 - eV > 1000kT$  at low injection levels. At high injection levels, the moving  $\nu_2$  peak swamps the stationary one at  $\nu_1$ . At low current densities the carriers seem to acquire extra energy from the applied field. The excess energy is far too large to be accounted for by thermal excitation.

A high-order process such as an Auger process cannot account for the relatively high quantum efficiency of such emission, so that we still lack a model able to explain the injection responsible for the "stationary" emission.

## VI. CONCLUSION AND SUMMARY

In order to determine the nature of the injection mechanisms which are responsible for the electro-

luminescence in GaAs  $p$ - $n$  junctions, we have performed a series of investigations examining the behavior of the different luminescence peaks as a function of injection level, doping level, doping gradient, dopant, and temperature. Three injection mechanisms seem to be operative in giving off radiation at near band-gap energies. Models for two of these are proposed and tested. The nature of the third emission remains an open question.

The behavior of the three emission mechanisms is summarized below.

(1) *Stationary peaks* generally seen in diodes with low donor concentration. In the diodes in which they are present their intensity increases with temperature. Some of these peaks are very near the absorption edge and may involve a bound exciton recombination as suggested by D. K. Wilson.<sup>23</sup>

This class of peaks presents the peculiarity of having its center photon energy higher than the applied voltage. Carriers may obtain their excess energy from the applied field or from thermal energy. Although the temperature dependence is consistent, qualitatively, with thermal excitation, the magnitude of the difference is much too large. The origin of this emission is left as an open question.

(2) *Fast moving peaks* generally appearing only at low injection levels. The shift in peak energy in some diodes varies from 1.17 up to 1.47 eV. As an impurity band that wide is very unlikely to occur one has to assume a shift in the energy of the band where the transition originates, with respect to the one where the transition terminates. This shift is determined by the applied voltage according to relation (1) from which we conclude that the initial and final states are on opposite sides of the junction. A possible way of relating those states and explaining relation (1) is to assume a tunneling-assisted radiative transition. This model assignment is strengthened by the observed dependence of the logarithmic  $\mathcal{J}$  versus  $V$  slope on the diode width constant. The term "diagonal tunneling" is suggested to describe this phenomenon.

(3) *Slow moving peaks*. This is probably the most important emission since laser action almost always involves this transition. This emission is always present and is usually the dominant one. At high donor concentration, it has no phonon satellites but at lower donor concentrations, it has almost always one or two phonon satellites.

The data seem to be consistent with a band-filling model. The feature distinguishing this radiation from that involving a "diagonal tunneling" is the dependence of the logarithmic slope of the  $\mathcal{J}$  versus  $V$  plot on the impurity concentration.

<sup>23</sup> D. K. Wilson, Appl. Phys. Letters 3, 129 (1963).